Kinetics of Cdc42 Membrane Extraction by Rho-GDI Monitored by Real-Time Fluorescence Resonance Energy Transfer†

Tyzoon K. Nomanbhoy,‡ Jon W. Erickson, and Richard A. Cerione*

Departments of Biochemistry, Molecular, and Cell Biology, and of Molecular Medicine, Cornell University, Ithaca, New York 14853

Received September 11, 1998; Revised Manuscript Received December 2, 1998

ABSTRACT: The mechanisms underlying the ability of the Rho-GDP dissociation inhibitor (RhoGDI) to elicit the release of Rho-related GTP-binding proteins from membranes is currently unknown. In this report, we have set out to address this issue by using fluorescence resonance energy transfer approaches to examine the functional interactions of the RhoGDI with membrane-associated Cdc42. Two fluorescence assays were developed to monitor the interactions between these proteins in real time. The first involved measurements of resonance energy transfer between *N*-methylanthraniloyl GDP (MantGDP) bound to Cdc42 and fluorescein maleimide covalently attached to cysteine 79 of RhoGDI (RhoGDI-FM). This assay allowed us to directly monitor the binding of RhoGDI to membrane-associated Cdc42. The second fluorescence assay involved measurements of resonance energy transfer between membrane-associated Cdc42−MantGDP and hexadecyl(amino) fluorescein that was randomly inserted into the membrane bilayer. This assay enabled us to directly monitor the (GDI-induced) release of Cdc42 from membranes. Analyses of the rates of change in the fluorescence of Cdc42−MantGDP, which serves as a resonance energy transfer donor in both of these assays, as a function of RhoGDI concentration suggests a two-step mechanism to explain the ability of RhoGDI to stimulate the release of Cdc42 from membranes. Specifically, we propose that the GDI first binds rapidly to membrane-associated Cdc42 and then a slower isomerization occurs which represents the rate-limiting step for the dissociation of the Cdc42−RhoGDI complex from membranes. We propose that this slow step in the observed kinetics reflects the time-course of translocation of the geranyl−geranyl lipid tail of Cdc42 from the outer leaflet of the membrane to the isoprenyl binding site observed in the previously reported NMR structure of the Cdc42−RhoGDI complex [Gosser et al. (1997) *Nature 387,* 814].

The Ras-like low molecular weight GTP-binding proteins form a superfamily whose members are involved in a variety of biological pathways which include the regulation of cell growth and differentiation, vesicular transport, and cytoskeletal organization (*1*). A major interest of our laboratory has been directed toward studying the molecular regulation and biochemical activities of one such GTP-binding protein, Cdc42, which is a member of the Rho subfamily of the Ras superfamily. Other members of this subfamily include the Rho (A, B, C, D, and G) and Rac (1 and 2) proteins. In mammalian cells, these proteins have been implicated in several diverse pathways, including the organization of the actin cytoskeleton (*2*, *3*), the activation of nuclear (stress-regulated) MAP kinases (*4*−*8*), and cell cycle progression (*9*). Overall, a number of lines of evidence now argue that the Rho subfamily proteins play critical roles in the maintenance of proper cell growth and development.

Like other GTP-binding proteins, Cdc42 exists in either an active GTP-bound state or an inactive GDP-bound state, as determined by a tightly regulated GTP-binding/GTPase cycle. Regulators of the GTP-binding/GTPase cycle of Cdc42 and related proteins include guanine nucleotide exchange factors (GEFs), which catalyze the exchange of GDP for GTP, GTPase-activating proteins (GAPs), which stimulate the hydrolysis of GTP to GDP, and GDP dissociation inhibitors (GDIs).

A GDI activity for Cdc42 was purified from brain cytosol (*10*), and through protein microsequencing was shown to be identical to the GDI previously identified for the RhoA protein [designated RhoGDI (*11, 12*)]. It was subsequently shown that RhoGDI could also interact with GTP-bound Cdc42 and inhibit both intrinsic and GAP-stimulated GTP hydrolysis (*13*). In addition, RhoGDI was shown to interact with membrane-associated Cdc42 and promote its dissociation from membranes (*11*). It is now known that RhoGDI exhibits these three activities toward Rac and RhoA, as well as Cdc42. Recently, it has been shown that the insert region which is unique to Rho-related proteins (residues 120−132 in Cdc42) is essential for the GDI-induced inhibition of GDP dissociation and GTP hydrolysis but not for its membrane-releasing activity (*14*). Thus, despite the suspected physiological importance of the membrane-releasing activity of RhoGDI, the mechanism by which this activity is mediated is still poorly understood.

† This work was supported by Grants GM47458 and EY06429 from the National Institutes of Health.

* To whom correspondence should be addressed at Dept. of Molecular Medicine, VMC, Cornell University, Ithaca, NY 14853.

‡ Present address: The Scripps Research Institute, The Skaggs Institute of Chemical Biology, 10550 North Torrey Pines Road, La Jolla, CA 92037.

10.1021/bi982198u CCC: $18.00
Published on Web 01/16/1999

To begin to determine how the RhoGDI triggers the release of Rho-related GTP-binding proteins from membranes, we have developed two types of fluorescence assays to monitor the interactions between RhoGDI and membrane-associated Cdc42. One assay involves directly monitoring the binding of RhoGDI to Cdc42 using resonance energy transfer. In this assay, Cdc42 is loaded with a fluorescent GDP analogue (MantGDP) and inserted into plasma membranes. Resonance energy transfer is then used to follow the binding of RhoGDI molecules, labeled at a single cysteine residue (Cys79) with fluorescein maleimide (RhoGDI-FM), to the membrane-associated Cdc42−MantGDP complex. The second assay allows us to monitor the GDI-induced release of Cdc42 from membranes. In this case, the loss of resonance energy transfer between the membrane-associated Cdc42−MantGDP and the fluorescent lipid, hexadecyl(amino) fluorescein (HAF), randomly inserted into plasma membranes, is used to monitor the (GDI-induced) dissociation of Cdc42−MantGDP from membranes in real time. On the basis of the analyses of Cdc42/RhoGDI interactions using these fluorescence assays, we can describe the GDI-induced release of Cdc42 from membranes in terms of a relatively simple, two-step binding model.

EXPERIMENTAL PROCEDURES

Proteins. RhoGDI was expressed as a GST fusion protein in *Escherichia coli*, and Cdc42 was expressed in *Spodoptera frugiperda* (Sf21) using previously described procedures (*15*).

MantGDP. The MantGDP used in this study was synthesized from *N*-methylisatoic anhydride (Molecular Probes) and GDP (Sigma) using a protocol essentially similar to the published procedures (*16, 17*), with the following modifications. First, the Mant-derivatized nucleotide was separated from free anhydride and unlabeled GDP by chromatography on Q Sepharose instead of DEAE Sepharose. Second, we used a 0.2−1 M triethylamine bicarbonate (TEAB) gradient to elute MantGDP from the column, instead of a 0.2−0.5 M TEAB gradient. The resulting MantGDP, when complexed to Cdc42, was only slightly quenched upon the binding of RhoGDI (∼3−5%).

For the preparation of isoprenylated Cdc42 complexed to MantGDP, isoprenylated GST-Cdc42 was first bound to glutathione agarose beads. The beads were then incubated with EDTA (final concentration = 10 mM) and MantGDP (final concentration = 200 μM) for twenty minutes at room temperature. $MgCl_2$ was then added to a final concentration of 20 mM to block the further exchange of nucleotide onto Cdc42. The beads were washed with Buffer FM (20 mM Tris-HCl, pH 8.0, 2 mM $MgCl_2$, 50 mM NaCl) to remove free Mant nucleotide, and then the GST-Cdc42 was eluted from the glutathione−agarose beads using Buffer FM containing 10 mM glutathione and the GST moiety was released through thrombin digestion.

For the preparation of RhoGDI conjugated with fluorescein maleimide (RhoGDI-FM), RhoGDI was first incubated with 0.5 mM fluorescein maleimide (Molecular Probes) for 60 min at room temperature in the dark. The reaction was terminated by the addition of DTT to 10 mM. The conjugated protein was separated from the free probe by elution through a PD-10 desalting column (Pharmacia).

Fluorescence Measurements with Membrane-Vesicle Preparations. Plasma membranes were purified from uninfected Sf21 insect cells, using a modification of the Thom procedure (*18*). Briefly, insect cells were harvested by centrifugation, and the cell pellet was resuspended into ∼5 mL of Ca^{2+}- and Mg^{2+}-free Hanks medium and lysed by Dounce homogenization. The lysate was diluted into about 80 mL of extraction buffer (20 mM sodium borate, pH 10.2, 0.1 mM EDTA). This was placed on a rocker at 4 °C for 15 min and subsequently spun at 500 rpm for 10 min in a swinging bucket rotor. The supernatant was collected, and the membranes in the supernatant were pelleted by centrifugation at 15 000 rpm for 20 min. The membranes were then resuspended in 20 mM Hepes, pH 7.4, and used to overlay a 1 mL 39%/35% sucrose step gradient. This was centrifuged at 30 000 rpm for 60 min in an SW41 rotor. The membranes were collected at the sucrose/aqueous interface and stored at 4 °C.

For insertion of Cdc42 into the lipid bilayer, 100 μL of plasma membranes (∼4 mg of a phospholipid/protein mixture), prepared as described above, was pelleted by centrifugation at 14 000 rpm for 10 minutes. The supernatant was removed, and ∼400 pmol of Cdc42−MantGDP was added to the membranes. In experiments in which resonance energy transfer was carried out between Cdc42 and membranes, Cdc42−MantGDP was added to membranes together with 10 μM hexadecyl(amino) fluorescein (HAF). Cdc42−MantGDP (or Cdc42−MantGDP and HAF) was incubated with membranes for 30 min at room temperature, after which the membranes were pelleted by centrifugation at 14 000 rpm in a microfuge. The membranes were washed four times with Buffer FM to remove proteins nonspecifically associated with membranes. After the final wash, the pellet was resuspended in 200 μL of Buffer FM.

Fluorescence Spectroscopy. The fluorescence measurements were made using an SLM 8000c spectrofluorometer operated in the photon-counting mode. Samples were stirred continuously and thermostated at 20 °C in Buffer FM.

Data Analysis. To obtain an initial characterization of the rate of observed fluorescence changes, we analyzed the first 100 seconds of the quenching of Cdc42−MantGDP fluorescence by RhoGDI-FM empirically using the following equation:

$$F(t) = F_f + Ae^{-k_{app1}t} + Be^{-k_{app2}t} \quad (1)$$

where $F(t)$ is the fluorescence at time t, F_f is the final fluorescence, A is the pre-exponential term of the slow component of the fluorescence quenching, k_{app1} is the apparent rate constant of the slow component, B is the pre-exponential factor of the fast component of the fluorescence quenching, and k_{app2} is the apparent rate constant of the fast component. In fitting the data, the value of F_f was estimated from the predetermined K_d value for the interaction between RhoGDI and membrane-associated Cdc42, and was fixed. In addition, the values that could be adopted by A and B were constrained such that the sum ($F_f + A + B$) would equal the initial fluorescence. The only parameters that were allowed to vary freely were the values for k_{app1} and k_{app2}, and these were determined by convergence for each concentration of RhoGDI.

The RhoGDI-dependent release of Cdc42−MantGDP from membranes and the accompanying reversal of energy transfer between Cdc42−MantGDP and HAF were initially ap-

proximated by using the following equation to fit the first 100 s of the increase of Mant fluorescence:

$$F(t) = F_f + Ce^{-k_{app3}t} \quad (2)$$

where $F(t)$ is the fluorescence at time t, F_f is the final fluorescence, C is the pre-exponential factor, and k_{app3} is the apparent rate constant. In obtaining the fits for each concentration of RhoGDI, F_f and C were constrained such that the sum of $(F_f + C)$ would equal the initial fluorescence.

Determination of the Rate Constants for the Interaction between RhoGDI and Membrane-Associated Cdc42. For a more complete description of the interaction between RhoGDI and Cdc42, the full analytical expression resulting from applying the following scheme was derived:

$$R + C \underset{k_2}{\overset{k_1}{\rightleftharpoons}} \text{RC-1 (fast)}$$

$$\text{RC-1} \underset{k_4}{\overset{k_3}{\rightleftharpoons}} \text{RC-2 (slow)}$$

where R corresponds to RhoGDI, C corresponds to Cdc42, RC-1 corresponds to an intermediate state of the RhoGDI−Cdc42 complex, and RC-2 corresponds to the final state of the RhoGDI−Cdc42 complex.

We first estimated $(k_3 + k_4)$, as this value would correspond to the apparent rate constant for the release of Cdc42 from membranes (k_{app3}), at saturating concentrations of RhoGDI (*19*). We determined this value to be 0.133 s^{-1} from the y-intercept of a linear fit of a plot of $1/k_{app3}$ versus 1/[RhoGDI] (data not shown). The rate of formation of RC-1 and RC-2 may be written respectively as follows:

$$\frac{d[RC\text{-}1]}{dt} = k_1[R][C] + k_4[RC\text{-}2] - (k_2 + k_3)[RC\text{-}1] \quad (3)$$

$$\frac{d[RC\text{-}2]}{dt} = k_3[RC\text{-}1] - k_4[RC\text{-}2] \quad (4)$$

Assuming steady-state conditions (i.e., $d[RC\text{-}1]/dt = 0$), and $[RC\text{-}2]/[RC\text{-}1] = k_3/k_4$,

$$dt = d[RC\text{-}2] \Big/ \left[\left(\frac{k_3k_1}{k_2 + k_3}\right)\left(\frac{k_4}{k_3} + 1\right)^2 [RC\text{-}2]^2 + \left\{\left(\frac{k_3k_4}{k_2 + k_3} - k_4\right) - \left(\frac{k_4}{k_3} + 1\right)([R_T] + [C_T])\right\}[RC\text{-}2] + \left(\frac{k_3k_1}{k_2 + k_3}\right)[R_T][C_T]\right] \quad (5)$$

where $[R_T]$ = total [RhoGDI] and $[C_T]$ = total [Cdc42]. Integration from [RC-2] = 0 at time $t = 0$, to [RC-2] = [RC-2(t)] at time $t = t$, followed by rearrangement yields the following expression, as adopted from a treatment described by Erickson et al. (*20*).

$$\frac{[RC - 2(t)]}{[C_T]} = \frac{b(\alpha e^{t\beta} - 1) + \beta(\alpha e^{t\beta} + 1)}{2c(1 - \alpha e^{t\beta})[C_T]} \quad (6)$$

where

$$a = (k_3k_1/(k_2 + k_3))[R_T][C_T]$$

$$b = (k_3k_4/(k_2 + k_3) - k_4) - (k_4/k_3 + 1)([R_T] + [C_T])$$

$$c = (k_3k_1/(k_2 + k_3))(k_4/k_3 + 1)^2$$

$$\alpha = (2c[C_T] + b - \beta)/(2c[C_T] + b + \beta)$$

$$\beta = (b^2 - 4ac)^{1/2}$$

Normalized data sets which visualized the release of Cdc42 from membranes, for concentrations of RhoGDI ranging from 74 to 260 nM, were fit to eq 6, constraining k_3 and k_4 such that $(k_3 + k_4) = 0.133\ s^{-1}$.

RESULTS

Resonance Energy Transfer as a Read-Out for the Binding of RhoGDI to Soluble and Membrane-Associated Cdc42. An important first step in these studies was to develop a resonance energy transfer assay for monitoring the direct interactions between Cdc42 and RhoGDI. We were able to do this by using a preparation of MantGDP, whose fluorescence was not significantly affected by the binding of unlabeled RhoGDI, as a fluorescence resonance energy transfer donor. The absorption capability of fluorescein maleimide, attached to Cys^{79} of RhoGDI (RhoGDI-FM; 1 ± 0.1 mol of FM per mol of RhoGDI), served as an energy transfer acceptor (*21*). The binding of RhoGDI-FM to Cdc42−MantGDP should then allow the FM moiety to gain sufficient proximity to the Mant nucleotide to enable resonance energy transfer between these chromophores, as read-out by a quenching of the MantGDP fluorescence [see Figure 1A; note that when starting with membrane-associated Cdc42−MantGDP, the release of Cdc42 from the membranes is the ultimate outcome of the binding of RhoGDI-FM (also see below)].

The data in Figure 1B shows the results of such an experiment performed in solution. In this case, the binding of RhoGDI-FM to Cdc42−MantGDP resulted in an immediate quenching of the MantGDP fluorescence (due to resonance energy transfer to the FM moiety attached to RhoGDI) that was complete within the time period of mixing, that is, less than 10 s. This quenching required that Cdc42 was isoprenylated, such that the fluorescence of *E. coli*-expressed Cdc42−MantGDP was not quenched by RhoGDI-FM, consistent with the requirement of the isoprenoid moiety on Cdc42 for its ability to bind the GDI with high affinity (*15*). Figure 1C shows the results of an identical experiment, except that the Cdc42−MantGDP was first inserted into purified plasma membranes. In this case, the rate at which the RhoGDI-FM quenched the MantGDP fluorescence was significantly reduced. This suggested that the association of Cdc42 with membranes kinetically impaired one or more steps in the overall reaction pathway between RhoGDI and Cdc42. Analyses of the binding profiles for the interactions between Cdc42−MantGDP and RhoGDI-FM in solution and for membrane-associated Cdc42 yielded apparent K_d values of ~2 nM for both cases (data not shown). Thus, the overall binding affinity of RhoGDI for Cdc42 did not appear to be significantly altered by its association with membranes. However, the difference in the kinetics of the quenching of Cdc42−MantGDP fluorescence by RhoGDI-FM, when Cdc42

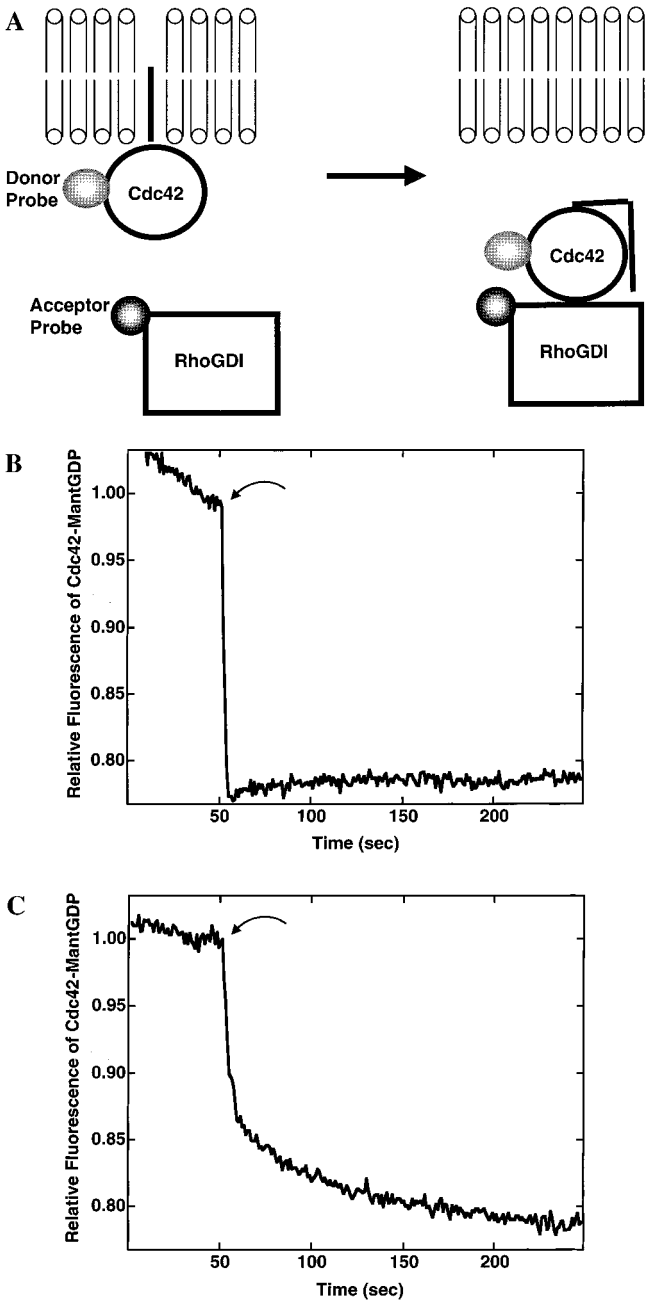

FIGURE 1: The interactions between Cdc42−MantGDP and RhoGDI-FM. (A) Presents a depiction of the binding interaction between Cdc42−MantGDP and RhoGDI-FM. Cdc42−MantGDP (17 nM), either solubilized (B), or membrane-associated (C), was incubated in buffer FM, and then the Mant fluorescence was observed (excitation = 350 nm, emission = 440 nm). At the indicated time (arrow), RhoGDI-FM was added to 60 nM.

is soluble versus membrane-associated, appears to be coupled to the RhoGDI-mediated release of Cdc42 from membranes (see below).

An Examination of the Rates of the Interaction between RhoGDI-FM and Membrane-Associated Cdc42−MantGDP. We next examined how the rate of quenching of MantGDP fluorescence, for Cdc42−MantGDP that was initially associated with membranes, was affected by different concentrations of RhoGDI-FM. The data shown in Figure 2 was fit to a double-exponential decay curve (eq 1 in Experimental Procedures), because the quenching of the Cdc42−MantGDP fluorescence by RhoGDI-FM was biphasic. The apparent rate

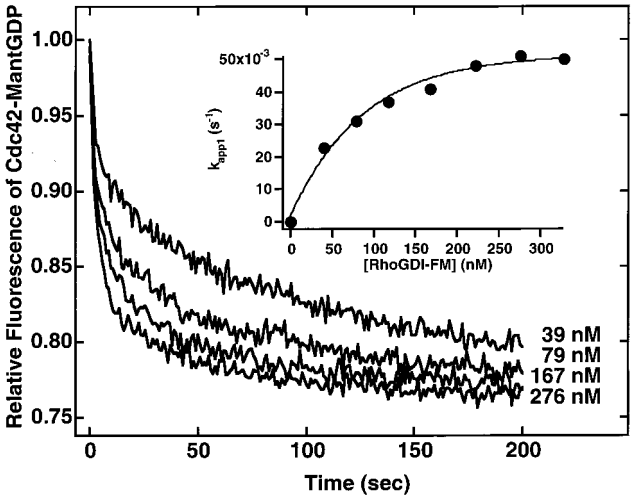

FIGURE 2: Kinetic analysis of the interaction between membrane-associated Cdc42−MantGDP and RhoGDI-FM. Membrane-associated Cdc42−MantGDP (31 nM) was incubated in Buffer FM, and the Mant fluorescence was observed (excitation = 350 nm, emission = 440 nm). At $t = 0$, different levels of RhoGDI-FM, as indicated to the right of the traces, were added, and the fluorescence quenching was monitored for 200 s after the addition of RhoGDI-FM. The fluorescence traces were analyzed by double-exponential fits as described in the Experimental Procedures and Results sections. Insert: For each RhoGDI concentration, the apparent rate constant obtained for the slow component of the double-exponential fit was plotted versus the RhoGDI concentration.

constants for the slow phase of the quenching showed a hyperbolic dependence on the RhoGDI concentration (Figure 2, insert) with half-maximal quenching occurring at 60 nM. The fact that the quenching of the Cdc42−MantGDP by RhoGDI is biphasic indicates that this interaction involves at least two discernible steps. The hyperbolic dependence of the apparent rate constants for the slow phase is consistent with a model in which a second-order binding step is followed by a (slower) first-order isomerization of the Cdc42−MantGDP/RhoGDI-FM complex (*19*).

A real-time assay for directly monitoring the GDI-induced release of Cdc42 from membranes was developed using resonance energy transfer. To do this, we inserted Cdc42−MantGDP into purified plasma membranes which contained the fluorescent lipid molecule, hexadecyl(amino) fluorescein (HAF), randomly distributed throughout the lipid bilayer. The idea was that, due to resonance energy transfer between Cdc42−MantGDP and HAF, the fluorescence of MantGDP bound to membrane-associated Cdc42 would be quenched. Upon the addition of RhoGDI, there then should be an increase in MantGDP fluorescence (i.e. a reversal of the energy transfer), due to the GDI-induced release of Cdc42−MantGDP from the HAF-containing membranes (as schematized in Figure 3A). Figure 3B shows the results of an experiment where different levels of RhoGDI were added to a fixed amount of membrane-associated Cdc42−MantGDP, in the presence of HAF. The RhoGDI-induced increases in Cdc42−MantGDP fluorescence, which specifically accompanied the release of the GTP-binding protein from HAF-containing membranes (but not from control membranes lacking the HAF resonance energy transfer acceptor probe), were examined at different levels of RhoGDI. Under these conditions, essentially all of the membrane-associated Cdc42 appeared to be released from the membranes by the RhoGDI. The data could be fit to a

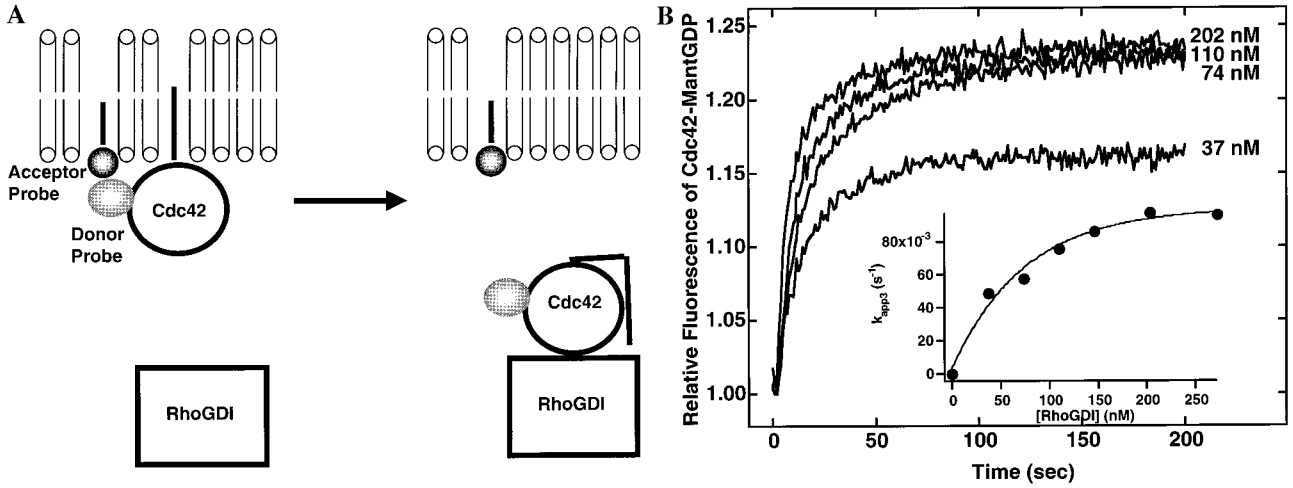

FIGURE 3: Kinetic analysis of the RhoGDI-dependent release of Cdc42 from membranes. (A) A depiction of the RhoGDI-induced release of Cdc42−MantGDP from HAF-containing membranes. (B) Cdc42−MantGDP (31 nM), inserted into membranes containing HAF, was incubated in Buffer FM, and Mant fluorescence was observed (excitation = 350 nm, emission = 440 nm). At $t = 0$, different levels of RhoGDI, as indicated to the right of the traces, were added, and the fluorescence increase was monitored for 200 s after the addition of RhoGDI. The fluorescence traces were analyzed by single-exponential fits as described in the Experimental Procedures and Results sections. Insert: For each RhoGDI concentration, the apparent rate constant obtained was plotted versus the RhoGDI concentration.

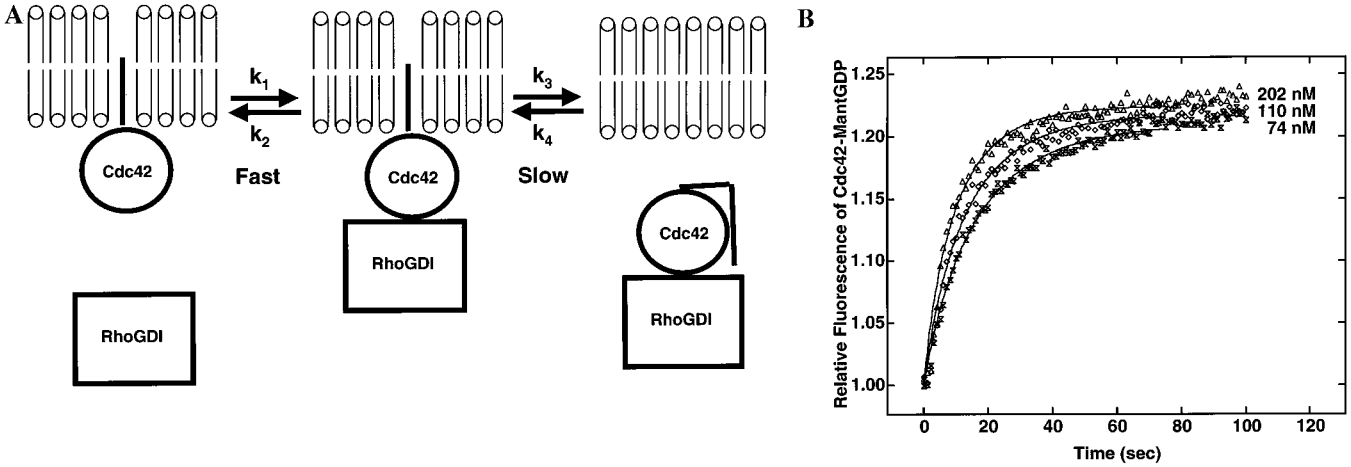

FIGURE 4: Description of Cdc42/RhoGDI interactions as a two-step model. (A) Depiction of the binding of RhoGDI to Cdc42 and its subsequent release from membranes. (B) Fits to the fluorescence data monitoring the Rho-GDI-induced release of Cdc42 from membranes using eq 6 (see Experimental Procedures).

single exponential (eq 2 in Experimental Procedures). When the apparent rate constants for the data were plotted as a function of RhoGDI concentration (Figure 3B, insert), a hyperbolic dependence on RhoGDI concentration was obtained with half-maximal effects occurring at 52 nM, similar to what was observed when monitoring the slow phase for Cdc42−MantGDP/RhoGDI-FM interactions.

A Model Describing the Interaction between RhoGDI and Membrane-Associated Cdc42. The biphasic quenching by RhoGDI-FM of membrane-bound Cdc42−MantGDP fluorescence, together with the similarities in the rates for the slow phase of the quenching and for the enhancement of Cdc42−MantGDP fluorescence due to its release from membranes, suggests a two-step model for the interaction between RhoGDI and membrane-associated Cdc42 (Figure 4A). In this model RhoGDI first binds to membrane-associated Cdc42 to form the intermediate Cdc42−RhoGDI complex. This step occurs relatively fast (forward rate constant = k_1) and would represent the fast phase of the quenching of the Cdc42−MantGDP fluorescence, due to energy transfer to FM-labeled RhoGDI. The second step represents an isomerization of the Cdc42−RhoGDI complex (forward rate = k_3), as reflected by the slow phase of the quenching of Cdc42−MantGDP fluorescence. This conformational change within the Cdc42−RhoGDI complex apparently increases the proximity between the Mant and fluorescein moieties. We would suggest that the rate for this conformational change is significantly decreased when Cdc42 is membrane-associated (see below) and that it corresponds to the rate-limiting step for the release of Cdc42 from membranes.

We have fit the data for the release of Cdc42−MantGDP from membranes (Figure 3B) as described in Experimental Procedures, using eq 6. We selected this set of data, rather than the data which monitored the binding of RhoGDI to membrane-associated Cdc42, because the former set of data visualized a single event (i.e., the release of Cdc42 from membranes), while the latter apparently visualizes multiple events. The fits to the experimental data, for RhoGDI concentrations ranging from 74 to 202 nM, are shown in Figure 4B. Fits were also carried out for 165 and 260 nM RhoGDI (Table 1). Overall, we find that that the two-step

Table 1

[RhoGDI] (nM)	rate constants				
	k_1 (M^{-1} s^{-1})	k_2 (s^{-1})	k_3 (s^{-1})	k_4 (s^{-1})	K_d (nM)
74	1.51×10^6	0.47	0.13	0.003	6.9
110	1.50×10^6	0.51	0.13	0.003	7.7
165	1.20×10^6	0.42	0.13	0.003	7.9
202	1.57×10^6	0.71	0.13	0.003	10.2
262	1.09×10^6	0.49	0.13	0.003	9.2

model for RhoGDI interactions with Cdc42 and its subsequent release from membranes describe the data well and yield rate constants that do not significantly vary over the entire range of RhoGDI concentrations examined (Table 1).

DISCUSSION

In this work, we set out to understand the mechanistic basis by which the RhoGDI mediates the release of Cdc42 and related Rho GTP-binding proteins from membranes, since this activity has been generally felt to be an essential aspect of the cellular regulation of these small GTP-binding proteins. We first developed an assay for the direct binding of RhoGDI to membrane-associated Cdc42 by monitoring the fluorescence resonance energy transfer between Cdc42−MantGDP and RhoGDI that was covalently modified at a single cysteine residue with fluorescein maleimide (RhoGDI-FM). We also established a real time assay for the RhoGDI-induced release of Cdc42 from membranes by measuring the loss in energy transfer between Cdc42−MantGDP and the fluorescent lipid hexadecyl(amino) fluorescein (HAF), which was randomly inserted into the membrane bilayer. The results obtained from these two assays are consistent with a simple model for the functional interactions between RhoGDI and membrane-associated Cdc42. The first step is the rapid binding of RhoGDI to Cdc42, followed by a slower isomerization of the Cdc42−RhoGDI complex. The rate of the second step for Cdc42/RhoGDI interactions in membranes is similar to the rate that we measure for the single-exponential increase in Cdc42−MantGDP fluorescence that represents the RhoGDI-induced release of Cdc42−MantGDP from HAF-containing membranes. Thus, the conformational change that occurs relatively slowly within the Cdc42−RhoGDI complex in membranes appears to be rate-limiting for the release of Cdc42 from the membrane bilayer.

We have considered other possible models to describe the functional interactions between RhoGDI and membrane-associated Cdc42; however, the predictions from these models were inconsistent with our results. For example, a simple bimolecular reaction describing the interaction between RhoGDI and membrane-associated Cdc42 predicts that the direct interaction between these proteins would yield a monophasic rather than a biphasic change in fluorescence resonance energy transfer. We have also considered a model in which membrane-associated Cdc42 exists in two conformations, of which only one conformation interacts with RhoGDI. The slow step in this model would be the isomerization between the two conformations of Cdc42. This model could explain a biphasic change in fluorescence resonance energy transfer for the direct interaction between Cdc42−MantGDP and RhoGDI-FM; however it also would require that the release of Cdc42 from membranes yields a biphasic increase in the fluorescence of Cdc42−MantGDP, which is not consistent with our results.

Thus, we feel that the two-step model described above provides the simplest explanation for the functional interactions of RhoGDI with the membrane-bound Cdc42. Further support for this comes from recent findings in our laboratory that amino-terminal truncated forms of GDI can still bind to Cdc42 but are not able to stimulate the release of Cdc42 from membranes (T. Nomanbhoy et al., data not shown). These truncated GDI molecules are apparently unable to trigger the isomerization within Cdc42 that is rate-limiting for membrane dissociation. At present, we do not know the molecular details underlying this conformational change. However, an attractive possibility is raised from recent NMR studies of the tertiary structure of the RhoGDI (*21*). These data argue that Cdc42 makes at least two contacts with RhoGDI. One occurs at the amino-terminal domain of RhoGDI and appears to be necessary for the GDI-induced inhibition of GDP dissociation from Cdc42. Recent results suggest that residues 120−132 of Cdc42, which make up an insert region that is unique to Rho proteins, may be involved in this interaction (*14*). A second contact between Cdc42 and RhoGDI appears to occur within the carboxyl-terminal domain of the GDI. It was proposed that the isoprene (geranyl−geranyl) moiety, attached to cysteine 188 of Cdc42, is buried in a hydrophobic pocket (4.5−5.5 Å wide, 9 Å long, and 10 Å deep) within the carboxyl-terminal portion of the RhoGDI molecule. Presumably it is this interaction that results in the release of Cdc42 from membranes. We would propose that the isomerization which is rate-limiting for the RhoGDI-mediated release of Cdc42 from membranes reflects the movement of the geranyl−geranyl moiety from the lipid milieu of the membrane into the hydrophobic pocket of the RhoGDI molecule. It is interesting that the rate of this conformational change appears to be dependent on whether Cdc42 is associated with membranes, such that the second step is not detectable when monitoring Cdc42/RhoGDI interactions by resonance energy transfer in solution, at least when using conventional mixing. If the rate-limiting isomerization reflects the insertion of the isoprene moiety into the hydrophobic pocket of RhoGDI, then it is not surprising that the interactions between the lipid bilayer and the isoprene moiety would slow the rate at which this GDI-induced conformational change occurs. Future studies will be directed at further characterizing the interactions between RhoGDI and membrane-associated Cdc42 and toward understanding how these interactions are regulated within cells.

ACKNOWLEDGMENT

We would like to thank R. Vazquez and Dr. R. E. Oswald for helpful discussions and Cindy Westmiller for expert technical assistance.

REFERENCES

1. Macara, I. G., Lounsbury, K. M., Richards, S. A., Mckiernan, C., and Bar-Sagi, D. (1996) *FASEB J. 10*, 625−630.
2. Kozma, R., Ahmed, S., Best, A., and Lim, L. (1995) *Mol. Cell Biol. 15* (4), 1942−1952.
3. Nobes, C. D., and Hall, A. (1995). *Cell 81*, 53−62.
4. Coso, O. A., Chiariello, M., Yu, J., Teramoto, H., Crespo, P., Xu, N., Miki, T., and Gutkind, J. S. (1995) *Cell 81*, 1137−1146.

5. Minden, A., Lin, A., Claret, F., Abo, A., and Karin, M. (1995) *Cell 81*, 1147−1157.
6. Hill, C. S., Wynne, J., and Treisman, R. (1995) *Cell 81*, 1159−1170.
7. Bagrodia, S., Derijard, B., Davis, R. J., and Cerione, R. A. (1995) *J. Biol. Chem. 270*, 27995−26062.
8. Zhang, S., Han, J., Sells, M. A., Chernoff, J., Knaus, U. G., Ulevitch, R. J., and Bokoch, G. M. (1995) *J. Biol. Chem. 270*, 23934−23936.
9. Olson, M. E., Ashworth, A., and Hall, A. (1995) *Science 269*, 1270−1272.
10. Leonard, D., Hart, M. J., Platko, J. V., Eva, A., Henzel, W., Evans, T., and Cerione, R. A. (1992) *J. Biol. Chem. 267*, 22860−22868.
11. Fukumoto, Y., Kaibuchi, K., Hori, Y., Fujioka, H., Araki, S., Ueda, T., Kikuchi, A., and Takai, Y. (1990) *Oncogene 5*, 1321−1328.
12. Ueda, T., Kikuchi, A., Ohga, N., Yamamoto, J., and Takai, Y. (1990) *J. Biol. Chem. 265*, 9373−9380.
13. Hart, M. J., Maru, Y., Leonard, D., Witte, O., Evans, T., and Cerione, R. A. (1992) *Science 258*, 812−815.
14. Wu, W. J., Leonard, D. A., Cerione, R. A., and Manor, D. (1997) *J. Biol. Chem. 272*, 26153−26158.
15. Nomanbhoy, T. K., and Cerione, R. A. (1996) *J. Biol. Chem. 271*, 10004−10009.
16. Hiratsuka, T. (1983) *Biochim. Biophys. Acta 742*, 496−508.
17. Leonard, D. A., Evans, T., Hart, M., Cerione, R. A., and Manor, D. (1994) *Biochemistry 33*, 12323−12328.
18. Thom, D., Powell, A. J., Lloyd, C. W., and Rees, D. A. (1977) *Biochem. J. 168*, 187−194.
19. Stickland, S., Palmer, G., and Massey, V. (1975) *J. Biol. Chem. 250*, 4048−4052.
20. Erickson, J. E., Goldstein, B., Holowka, D., and Baird, B. (1987) *Biophys. J. 52*, 657−662.
21. Gosser, Y. Q., Nomanbhoy, T. K., Aghazadeh, B., Manor, D., Combs, C., Cerione, R. A., and Rosen, M. K. (1997) *Nature 387*, 814−819.

BI982198U